Journal of the European Ceramic Society 15 (1995) 913–920

0955-2219(95)00039-9
0955-2219/95/$9.50

Effect of Mullite–Zirconia Additions on the Creep Behaviour of High-Alumina Refractories

C. Wolf,[a] R. Kauermann,[a] H. Hübner,[a] J. A. Rodrigues[b] & V. C. Pandolfelli[b]

[a]Arbeitsbereich Werkstoffphysik, Technische Universität Hamburg-Harburg, D-21071 Hamburg, Germany
[b]Departamento de Materiais, Universidade Federal de São Carlos, 13.565–905 São Carlos — SP, Brazil

(Received 20 December 1994; accepted 10 February 1995)

Abstract

The creep behaviour of high-alumina refractories containing increasing amounts of a fused mullite–zirconia aggregate (MZA) of eutectic composition was studied experimentally. The MZA has been added with the intention of improving the work of fracture and the thermal shock resistance through microcrack toughening. The creep resistance was found to decrease with increasing MZA content. This was attributed to the formation of an increasing fraction of a substructure composed of small grains and an amorphous binder phase situated between the large agglomerate particles. Creep deformation mainly occurred within these fine-grained interagglomerate regions, but rate controlled by mullite formation kinetics as an accommodation process. This interpretation is substantiated by the measured values of the stress exponent (n = 1·2–2·7) and the activation energy for creep ($Q \approx$ 720 kJ/mol) and by the finding that the creep rate was distinctly reduced by a preceding heat treatment.

1 Introduction

During the last decade, modern refractories have been developing into a class of highly sophisticated multiphase composite materials. As pointed out recently by Bradt[1] in a review on present day refractories, the manyfold and complex reactions between the constituents of the microstructure which are dynamic and transient in nature must be understood when a critical assessment of the physical and mechanical properties is to be obtained.

Among the mechanical properties of refractories, the deformation behaviour at high temperature under compressive load is of particular interest. Knowledge of the creep data of refractories is a prerequisite for selecting materials that exhibit a minimum of creep in a given application, as well as for establishing engineering design parameters for the construction of stoves and furnaces, as has been clearly demonstrated by Ainsworth and Kaniuk.[2] Furthermore, it has been pointed out by Evans *et al.*[3] that the availability of creep data is an indispensable basis when stresses and strains in refractory components and structures in service are to be calculated. By using the Θ projection concept developed by Evans and Wilshire[4] they demonstrated that the creep strength of refractories under service conditions can be extrapolated from the creep data determined in the laboratory within a limited range of test conditions.[3] Finally, the investigation of basic creep mechanisms is the key for developing new materials of improved creep resistance for use in refractory settings where creep is to be minimized.

A series of experimental creep studies on a variety of refractories of different compositions have been reported in the literature.[2, 5–13] It is generally recognized that creep of refractories is strongly affected by the microstructure. Fundamentally, there are three microstructural features which influence the creep behaviour, i.e. (1) the mineral content (size and distribution of the crystalline aggregates); (2) the flux content (amount, composition and distribution of the glassy phase), and (3) the apparent porosity.

The aim of the work presented here was to evaluate the creep behaviour of an experimental high-alumina refractory particularly designed for high thermal shock resistance.[14] To achieve this, different amounts of a mullite–zirconia aggregate (MZA) were added with the purpose of taking advantage of the zirconia toughening effect on room temperature mechanical properties. In fact, an increase in both the work of fracture and the retained strength after thermal shock was observed as the MZA content was increased, pointing at an increased microcrack density caused by the presence of zirconia particles.[14] Likewise, a pronounced loss of high-temperature strength was found to occur at 1400°C. This was attributed to increasing fractions of glassy phase

Table 1. Compositions of the refractory materials

Materials	*Grain size range (mm)*	*Composition (wt%)*				
Tabular alumina*	0·044–2	90	80	70	60	50
Calcined alumina†	<0·01	10	10	10	10	10
Mullite–zirconia aggregate	0·21–1	—	10	20	30	40

*T-60, Alcoa (Germany).
†APC-2011 SG, Alcoa (Brazil).

introduced by the MZA additive.[14] It was to be expected that the increase in glass phase content should also degrade the creep resistance of the material which was actually found in this paper.

2 Experimental Details

2.1 Materials and sample preparation

Five different high-alumina refractories were tested. These consisted of a basic mixture of a tabular and a calcined alumina to which varying amounts of a fused mullite–zirconia aggregate (MZA) have been added. The pressed bricks were fired at 1510°C for 12 h as indicated in Ref. 14. Table 1 shows the compositions of the materials tested, as well as their grain-size ranges. In the following, these five materials are identified by the weight fraction of their MZA content. Samples for compressive testing having dimensions of 20 × 20 × 40 mm^3 and 12 × 12 × 20 mm^3 were prepared by cutting blocks from the as-fired bricks and grinding them to the final dimensions. Specimens for microstructural examinations were ground and polished using a diamond paste down to a size of 1 μm. Micrographs were obtained by scanning electron microscopy on as-polished microsections.

2.2 Mechanical testing

Experimental techniques used in the literature for generating creep data are: (1) the refractoriness-under-load test (RUL test) where under a constant load and at a constant heating rate the temperature of the onset of plastic deformation is determined, and (2) compressive creep tests under constant load and temperature. Both techniques were applied in the present study. RUL tests were carried out according to DIN 51053 using a heating rate of 5°C/min and a compressive stress of 0·2 MPa.

Creep tests were performed in a constant-load creep machine in air at 1400°C and 3 MPa until failure occurred. Both as-received materials (all compositions) and samples annealed for 10 days at 1400°C (compositions 0, 10 and 30% MZA content) were tested. Stress change tests at 1400°C from 1 to 10 MPa and temperature change tests at 3 MPa from 1300 to 1450°C were made to obtain the stress exponent, n, and the activation energy for creep, Q, respectively (see eqn 1).

3 Results

3.1 Micrographic examinations

The microstructures of the five refractories studied in this work are shown in Figs 1 and 2. Figs 1(a) and (b) compare the materials without MZA and with 20% of MZA at a low magnification. In both micrographs, the large grains of tabular alumina prevail. These particles are considered to be rigid even under creep conditions and therefore do not contribute to the deformation. Between these large crystalline components, there is a substructure consisting of small grains and an amorphous binder phase. A fine-grained interaggregate substructure of similar appearance was also reported by Wiederhorn and Krause[13] in a magnesium–chromite refractory. The comparison of Figs 1(a) and (b) demonstrates that the volume fraction occupied by the interaggregate substructure is increased and that the grain size of the small grains within this substructure is decreased when MZA is added.

In Figs 2(a), (b) and (c), micrographs of the refractories containing 10, 20, and 40% of MZA

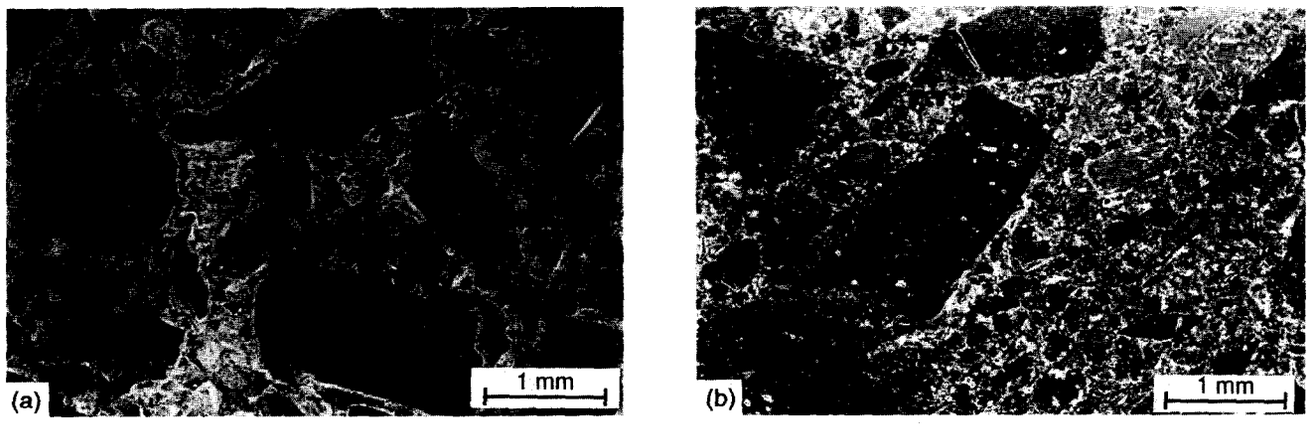

Fig. 1 SEM micrographs of refractories studied: (a) 0% of MZA content; (b) 20% of MZA content.

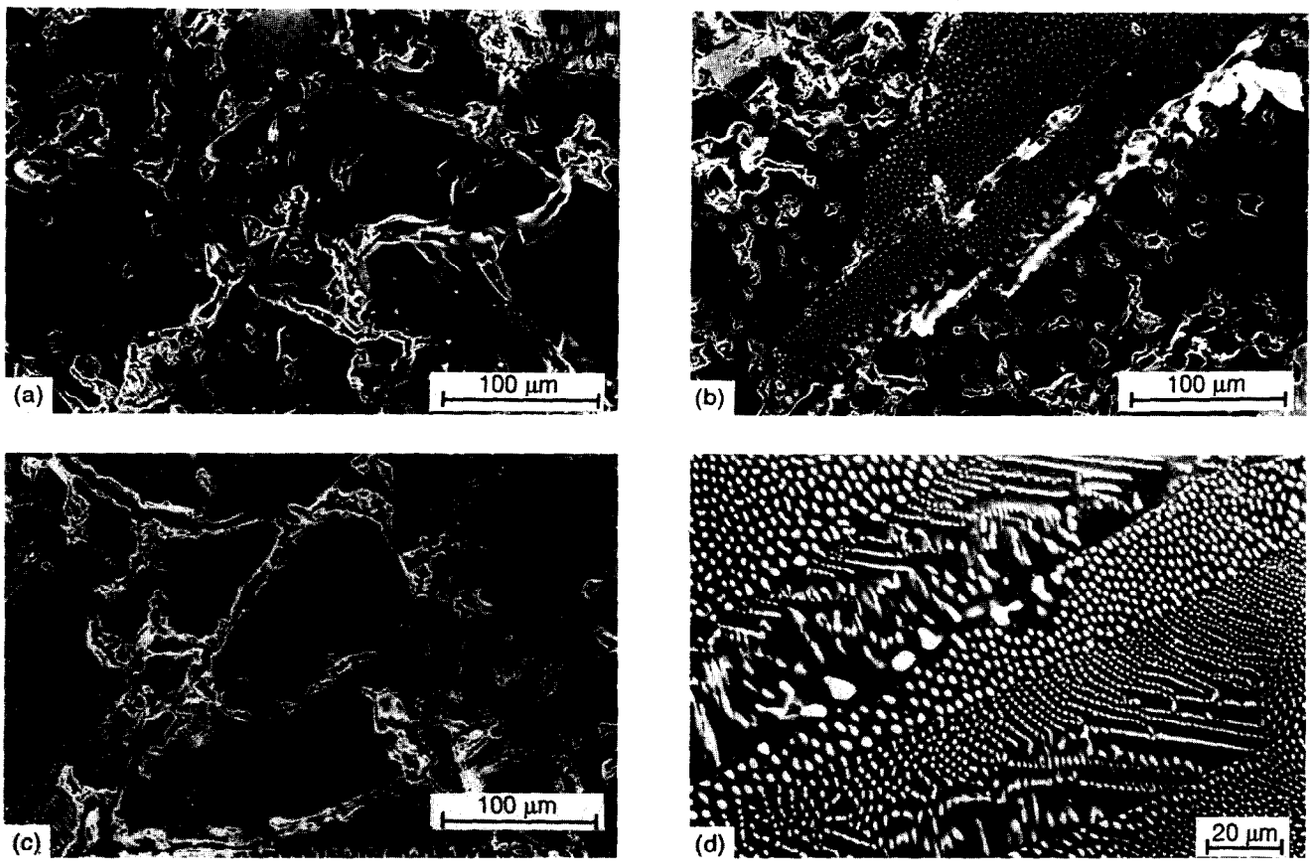

Fig. 2 Microstructure development with an increasing amount of MZA: (a) 10% of MZA content; (b) 20% of MZA content; (c) 40% of MZA content; (d) 20% of MZA content at higher magnification.

are shown at a higher magnification. The microstructure is composed of large particles of tabular alumina and the mullite–zirconia aggregate. These two components represent the major part of the crystalline phase content of the refractories.

The MZA can easily be detected in Fig. 2 by its dotted or striped appearance. The light phase is zirconia and the dark phase is mullite, as was proved by an EDX analysis. It is the mullite–zirconia eutectic which is formed in the Al_2O_3–SiO_2–ZrO_2 phase diagram. It has a eutectic temperature of 1750°C.[15] Within the MZA particles, the zirconia phase has a rod-like shape and forms periodic arrays of parallel orientation which are embedded in the continuous mullite matrix, as is shown in Fig. 2(d). This micrograph also demonstrates that there is a reasonable fit between the two phases of the eutectic since no microcracks can be detected within the MZA particles. However, considering the thermal expansion coefficients of mullite and zirconia, α_M and α_Z, ($\alpha_M = 5{\cdot}3 \times 10^{-6}\ K^{-1}$ and $\alpha_Z = 10{\cdot}0 \times 10^{-6}\ K^{-1}$ [16]), the value for the embedded phase is nearly twice that of the matrix phase. Thus, it may be concluded that thermally induced residual stress is created on cooling. In fact, evidence of microcrack formation at the ZrO_2/mullite interface was obtained on several micrographs.

Beside the rod-like zirconia component, there are also larger zirconia particles present in the micrographs of Figs 2(a), (b) and (c). These particles may be responsible for the toughening effect found in Ref. 14. Figures 2(a), (b), and (c) also show that the aggregate particles are surrounded by small layers of amorphous phase.

3.2 RUL tests

RUL test plots of the compositions 0, 20, and 40% MZA are presented in Fig. 3. The curves show a regime of linear thermal expansion and, at temperatures >1200°C, small deviations caused by the very onset of plastic deformation, the 20 and 40% materials going through a strain maximum at about 1400°C. According to DIN 51053, the upper temperature limit of the test is 1500°C and the softening temperature $T_{0{\cdot}5\%}$ is defined as that temperature where the compressive deformation attains a value of 0·5% with respect to the strain reached at the maximum. As can be seen from Fig. 3, $T_{0{\cdot}5\%} > 1500$°C for all compositions.

Since the sample deformation was very small when the temperature limit of 1500°C was reached the tests were continued at this temperature and stress for an additional 24 h to get a first idea of the creep resistance. By that means, creep curves $\epsilon(t)$ are developed which are also plotted in Fig. 3. From these curves the time $t_{0{\cdot}5\%}$ to reach a deformation $\epsilon = 0{\cdot}5\%$ was taken for each composition

Table 2. Comparison of mechanical properties at high temperatures

Aggregate (wt%)	*MOR* (MPa)*	$t_{0.5\%}$† *(h)*	ϵ_r‡ *(%)*	t_r‡ *(h)*	$\dot{\epsilon}_s$‡ *(s^{-1})*	$\dot{\epsilon}_{ann}$‡ *(s^{-1})*	*n*	*Q (kJ/mol)*
0	11·1	17	>10	>185·4	$1{\cdot}1 \times 10^{-7}$	—	1·3–2·0	692
10	8·5	—	7·63	6·3	$1{\cdot}7 \times 10^{-6}$	$4{\cdot}6 \times 10^{-7}$	1·7–2·7	668
20	6·8	3·9	6·06	2·2	$3{\cdot}9 \times 10^{-6}$	—	1·6–2·4	715
30	5·0	—	8·03	10·2	$1{\cdot}2 \times 10^{-6}$	6×10^{-7}	1·3–2·0	735
40	4·5	4·0	8·54	9·6	$1{\cdot}3 \times 10^{-6}$	—	1·2–2·1	778

* At 1400°C, Ref. 14.
† At 1500°C and 0·2 MPa.
‡ At 1400°C and 3 MPa.

and listed in Table 2. For the material without MZA content, this time is about 4 times that of the two other materials, indicating its superior creep resistance.

3.3 Creep tests

Creep curves plotted as creep rate $\dot{\epsilon}$ versus strain ϵ are shown in Fig. 4 for all materials in the as-received state at 1400°C and 3 MPa. The form of the creep curves is typical of many other ceramics and also refractories, exhibiting a primary, secondary or steady-state and tertiary creep stage. In some cases, no steady-state creep stage was found. The material without MZA had the lowest creep rate and did not exhibit any signs of creep damage up to ϵ = 10% where the test was stopped. The other compositions crept much more readily and exhibited failure by creep rupture at strains between 6 and 9%. Values of rupture strain ϵ_r, rupture time t_r and the steady-state or minimum creep rate $\dot{\epsilon}_s$ are listed in Table 2 for comparison.

The steady-state creep rate of a material is usually described by the equation

$$\dot{\epsilon}_s = A(S) \cdot \sigma^n \cdot \exp\left(-\frac{Q}{RT}\right), \qquad (1)$$

where $A(S)$ is a structure-dependent constant, σ is the stress, n is the stress exponent, Q is the activation energy for creep, and R and T have their usual meaning. To determine n and Q of eqn (1), stress and temperature change tests were performed. Examples of such tests are shown in Fig. 5 (stress changes) and Fig. 6 (temperature changes) for the refractory containing 30% of MZA. The stress exponent is calculated from the height of the $\dot{\epsilon}_s$ steps of Fig. 5 and the activation energy from the step height of Fig. 6. The n and Q values which were thus obtained are listed in Table 2.

The stationary creep rates measured at different stress levels at 1400°C are presented in Fig. 7 in a log–log plot. In this type of presentation, all five materials tested are close together, the difference increasing a little with increasing stress and reaching a factor of 5 at 10 MPa. The stress exponent derived from the slope of the curves has values between 1 and 2 and increases slightly with increasing applied stress level.

Figure 8 is an Arrhenius plot of the creep rates of the five materials at 3 MPa. Straight and nearly parallel lines were obtained which point at an activation energy for creep that is independent of temperature and equal for all compositions.

The effect of the MZA content on the steady-state creep rate at 1400°C and 3 MPa is shown in Fig. 9. It can clearly be recognized that the addition of MZA accelerates the creep deformation process. The maximum increase (by a factor of 25) was observed for the samples containing 20%

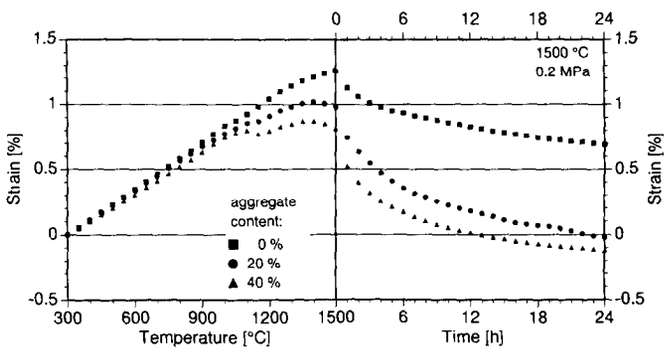

Fig. 3 RUL test plots.

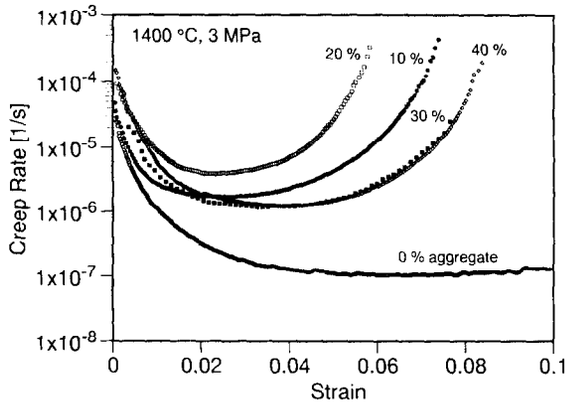

Fig. 4. Creep curves of high-alumina refractories in the as-received state.

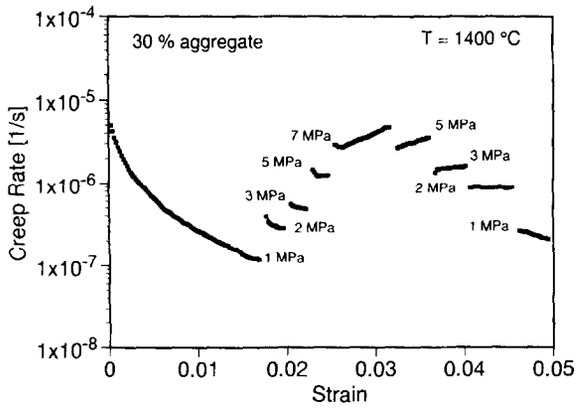

Fig. 5. Stress changes to determine the stress exponents, n.

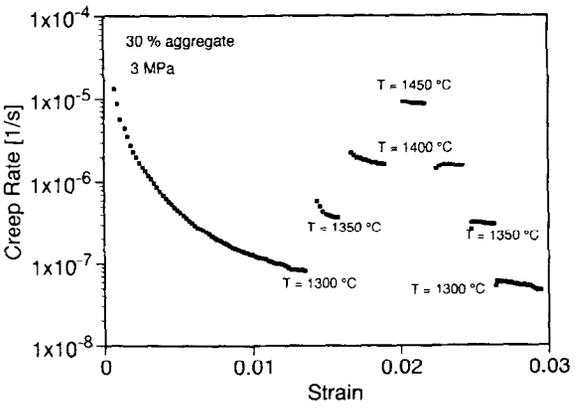

Fig. 6. Temperature changes to determine the activation energy for creep, Q.

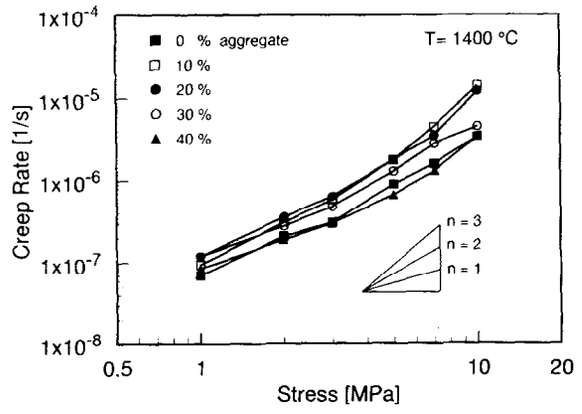

Fig. 7. Stress dependence of the stationary creep rate.

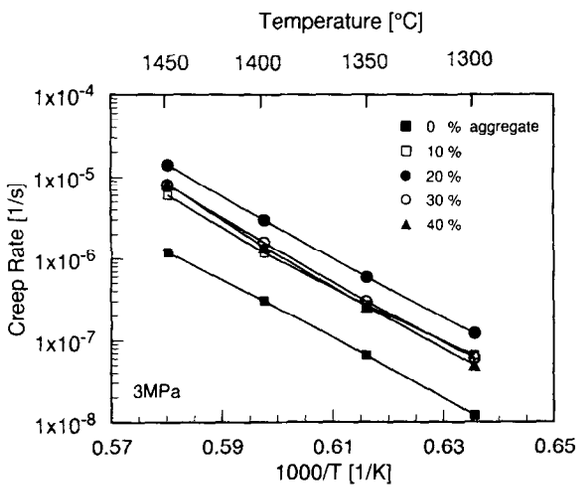

Fig. 8. Arrhenius diagram for the stationary creep rates.

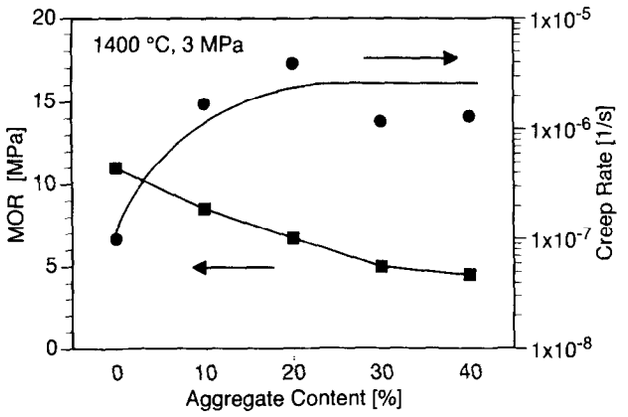

Fig. 9. Effect of MZA content on creep behaviour and high-temperature strength.

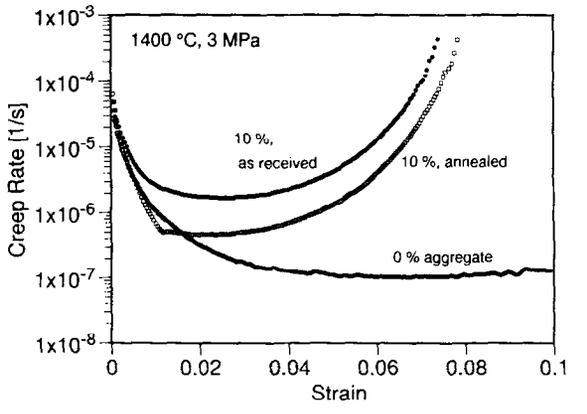

Fig. 10. Effect of heat treatment on the creep behaviour of 10% MZA refractory.

MZA. Figure 9 additionally contains modulus-of-rupture (MOR) data taken from Ref. 14. The MOR data are also listed in Table 2. The comparison of the two curves of Fig. 9 demonstrates that the high-temperature strength is degraded by the MZA addition in the same way that the creep rate is increased. From this finding it may be argued that the two mechanical parameters are controlled by the same microstructural features.

It has been reported by many investigators[5–7,10] that a post-fabrication heat treatment or hard firing condition reduces the creep rates of fired bricks. To examine the validity of this observation for the refractories studied here, compositions of 10 and 30% MZA were annealed at 1400°C for 10 days prior to creep testing. In Fig. 10 the creep curves of 10% MZA materials after the heat treatment and in the as-received state are compared. Minimum creep rate data of the two annealed

refractories are contained in Table 2. It was found that annealing altered the shape of the creep curve considerably, reducing minimum or steady-state creep rate by a factor of 4 in the material containing 10% and by a factor of 2 in the 30% MZA refractory.

4 Discussion

The creep behaviour of fired high-alumina refractories is strongly affected by their microstructure. There exists agreement in the literature that the two most important microstructural parameters are the crystalline phase content and the intergranular glassy phase. The results of the present research will be discussed in terms of these two features.

4.1 Crystalline phase content

According to the silica–alumina phase diagram, the equilibrium phases formed at elevated temperatures are mullite and corundum. Therefore, in high-alumina refractories mullite may be formed from alumina and excess silica by the reaction

$$3Al_3O_3 + 2SiO_2 \rightarrow 3\ Al_2O_3 \cdot 2SiO_2 \qquad (2)$$

The amount and morphology of the mullite phase controls the creep strength of high-alumina refractories since mullite formation increases the fraction of crystalline phases and reduces the amorphous phase content in the microstructure. Clements and Vyse[5] pointed out that best creep resistance is achieved when a three-dimensional network of mullite laths is present. Hulse and Pask[6] arrive at the same conclusion; namely that creep is controlled by the continuous mullite microstructure. Similar observations were made by Burdick and Day[7] and by Matsumara *et al.*[10] who found that all means of accelerating the rate of mullite formation resulted in a decrease of the creep rate. Other crystalline phases, such as large aggregate grains, are thought to be rigid and therefore do not contribute to the deformation. Furthermore, all four of these studies[5–7,10] agree upon the observation that the mullite content and hence the creep resistance of high-alumina refractories is increased through a heat treatment, either during initial firing or afterwards. A further observation concerning the effect of the crystalline phase content on the creep strength of refractories was made by Coath and Wilshire[9] and by Evans *et al.*[11] They reported that the creep rate of CaO/MgO doloma refractories decreased by up to an order of magnitude when the magnesia content was increased by admixing additional MgO powder to the raw material.

There is strong evidence that the creep behaviour of the refractories studied here is controlled by their mullite formation kinetics as well, as may be seen from the following arguments: (1) In metallographic observations a mullite lath network was observed at the interface between large alumina grains and MZA particles[14] where most of the local deformation is likely to occur. (2) The activation energy for creep is nearly the same for all five grades tested (Fig. 6). It has an average value of 720 kJ/mol and is very close to the activation energy for creep of mullite which has been reported to be 740 kJ/mol.[6] On the other hand, creep control by one of the other main constituents of the microstructure, i.e. the glassy phase and the large alumina grains, can be excluded since both of them have activation energies for creep much smaller than the measured figure of 720 kJ/mol. After Hulse and Pask,[6] silica-based glass has an activation energy in the range of 210–340 kJ/mol, whereas that of pure polycrystalline alumina is about 580 kJ/mol.[17] (3) The creep resistance was found to increase after a prolonged heat treatment (Fig. 8). This can be explained by temperature-activated mullite formation and silica consumption according to eqn (2). (4) Creep of the high-alumina refractories studied here is not a merely viscous process that would exhibit a stress exponent of $n = 1$. Instead, n values significantly greater than unity were found (Table 2 and Fig. 5). This finding indicates that the deformation additionally involves an accommodation process which probably actuates at the mullite–mullite and mullite–glass junctions and interfaces and which has a non-linear stress dependence.

4.2 Intergranular glassy phase

Even though the mullite phase is regarded to be rate-controlling in the creep of high-alumina refractories the properties of the glassy phase also affect the deformation behaviour. As pointed out by Hulse and Pask,[6] refractories with a high glass content will have a high deformation rate. Evidence of the effect of glassy phase content on the creep behaviour was also found in this study: (1) The MZA content caused the creep rate to be increased (Figs 2 and 7). This is attributed to an increased fraction of the amorphous phase in the microstructure because it was found in Ref. 14 that the addition of MZA resulted in an increased glass content. (2) In the presence of MZA, tertiary creep was observed to occur (Fig. 2) which is indicative of creep damage formed during deformation. The formation of creep damage generally decreases the rupture time t_r and reduces the ductility ϵ_r as indicated by the respective data in Table 2. It is well known that creep cavitation in

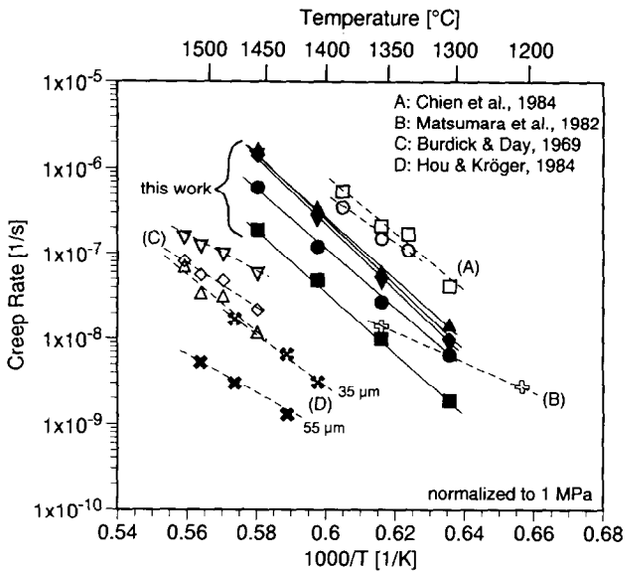

Fig. 11. Comparison of creep data from previous creep studies — data taken from Burdick and Day,[7] Matsumara *et al.*[10] Chien *et al.*,[19] and Hou and Kröger.[20]

structural ceramics is extraordinarily promoted by the presence of an amorphous phase. (3) The increase in creep rate and the decrease of rupture time must have the same origin. This follows from the fact that the $\dot{\epsilon}_s$ and t_r data of the four MZA containing refractories (Table 2) obey the Monkman–Grant relationship:[18]

$$\dot{\epsilon}_s \cdot t_r = \text{const.} \quad (3)$$

The $\dot{\epsilon}_s \cdot t_r$ product of the four data sets of Table 2 is about 0·040. The basic idea of the Monkman–Grant relationship is that, for a given failure mechanism, the strain at rupture is a constant.[18] Thus, if eqn (3) is valid for a given material, both the acceleration of the creep process and the reduction of the failure time are solely two different aspects of the same underlying mechanism. The Monkman–Grant relationship was found to hold for a series of glass-containing structural ceramics.[13]

The role of the intergranular glass phase in the creep of refractories was further elucidated by Wiederhorn and Krause.[13] They recognized that a substructure of small grains plus binder phase is present between the large rigid aggregate particles, and that it is this fine grain-size interaggregate microstructure which represents an easy path for dissolution and mass transport of the rate-controlling crystalline phase. After Ref. 13 the deformation occurs more easily within the fine grain-size bonding structure, leading to an effective interagglomerate viscosity of the bond phase that is smaller than in the absence of the fine interagglomerate grains. In the present investigation, evidence of increasing volume fractions of the fine grain-size interagglomerate microstructure with increasing MZA content were found in metallographic examinations as described in Section 3.1. This observation is taken as a further explanation of the decrease of the creep resistance due to the addition of MZA.

A further experimental result that emphasizes the role of the intergranular amorphous phase in the creep process of refractories is the work of Evans, Wilshire and co-workers.[9,11,12] In both CaO/MgO-based doloma refractories[9,11] and in magnesia refractories[12] it was observed that the creep rate increased drastically (up to a factor of 30) when the impurity level, specifically Fe_2O_3, was increased by intentional doping. It must be supposed that the Fe_2O_3 impurities were dissolved in the silicate-based glass phase. Due to its trivalent state, Fe^{3+} is known to substitute Si–Si bonds, thereby reducing the viscosity of the glass and accelerating the creep process.

4.3 Comparison with previous creep studies

In Fig. 11, the results of the present creep investigation are compared with creep data from previous creep studies. The comparison is limited to materials of similar basic compositions, i.e. other high-alumina refractories. Creep data of such materials were reported by Burdick and Day,[7] Matsumara *et al.*,[10] Chien *et al.*[19] and Hou and Kröger.[20]

To compare the results measured at different applied stresses, the data were normalized to a common stress of 1 MPa before plotting them in Fig. 11. For that, the stress exponent n given in the respective paper was used, or, if no stress exponent was indicated, $n = 1$ was assumed. As can be seen from Fig. 11, the creep data at a given temperature cover a range of about three orders of magnitude.

The spread of the data must be attributed to differences in both the grain size and glassy phase content of the various materials investigated. Unfortunately, the grain size is not reported in most of the papers, with the exception of Ref. 20 where creep rates of three different aluminas having grain sizes of 6, 35 and 55 μm, respectively, were measured. For the comparison of Fig. 11 the data of the 35 and 55 μm grain size material were selected since this figure is close to the lower limit of the grain-size range of the tabular alumina given in Table 1.

The glass-phase content of the high-alumina refractories studied in Refs 19 and 20 was 33–44% and 1%, respectively. For the refractories of the present investigation, a value between 10 and 20% seems to be a reasonable assumption. The creep data of these three studies are ranked in the same sequence in Fig. 11: the data sets of Refs 19 and

20 form the upper and lower boundary of the experimental data whereas the creep data of the present study are intermediate. Thus, it may be concluded that the fundamental microstructural feature that controls the creep rate of these refractories is the volume content of the glassy phase.

5 Conclusions

It was shown previously in Ref. 14 that the addition of a fused mullite–zirconia aggregate results in a considerable improvement of the work of fracture and the thermal shock resistance of high-alumina refractories. Unfortunately, high-temperature mechanical properties such as the strength and creep resistance are deteriorated by increasing amounts of MZA in the microstructure as is demonstrated by Fig. 9. Thus, to take full advantage of zirconia-induced microcrack toughening of the high-alumina refractories studied here, a balance must be achieved between the opposing influences of MZA on the mechanical properties. This may be obtained by optimizing the MZA content for a given application.

Acknowledgement

The authors are grateful to Magnesita, Alcoa, FAPESP, CNPq, and DAAD for providing materials and funds for this work. The authors also thank Professor R. C. Bradt for comments regarding the manuscript.

References

1 Bradt, R. C., Twenty first century refractories. In *Refractory Raw Materials and High Performance Refractory Products*, (Proceedings of the Second International Symposium on Refractories), eds Z. Xiangchong, L. Jiaquan, Y. Xingjian, & L. Maoqian. International Academic Publishers, Beijing, 1992, pp. 15–21; for a Chinese translation see: *J. Chinese Ceram. Soc.*, **21** (1993) 169–75.

2. Ainsworth, J. H. & Kaniuk, J. A., Creep of refractories in high temperature blast furnace stoves. *Am. Ceram. Soc. Bull.*, **57** (1978) 657–9.
3. Evans, R. W., Scharning, P. J. & Wilshire, B., Constitutive equations for creep of a fired doloma refractory. *Br. Ceram. Trans. J.*, **85** (1986) 63–5.
4. Evans, R. W. & Wilshire, B., *Creep of Metals and Alloys*. The Institute of Metals, London, 1984.
5. Clements, J. F. & Vyse, J., Creep measurements on some high-alumina refractories. *Trans. Brit. Ceram. Soc.*, **65** (1966) 59–85.
6. Hulse, C. O. & Pask, J. A., Analysis of deformation of a fireclay refractory. *J. Am. Ceram. Soc.*, **49** (1966) 312–18.
7. Burdick, V. L. & Day, D. E., Creep of high-alumina refractories. *Am. Ceram. Soc. Bull.*, **48** (1969) 1109–13.
8. Trostel, L. J., Deformation of oxide refractories. In *Deformation of Ceramics Materials*, eds R. C. Bradt & R. E. Tressler. Plenum Press, New York & London, 1974, pp. 339–60.
9. Coath, J. A. & Wilshire, B., The influence of variations in composition on the creep behaviour of doloma. *Ceramurgia Int.*, **4**, (1978) 66–70.
10. Matsumura, I., Hayashi, Y., Hiyama, Y. & Ijiri, A., Refractoriness under load and hot creep measurements. *Taikabutsu Overseas*, **2** (1982) 36–42.
11. Evans, R. W., Scharning, P. J. & Wilshire, B., Creep of CaO/MgO refractories. *J. Mater. Sci.*, **20** (1985) 4163–8.
12. Evans, R. W., Scharning, P. J. & Wilshire, B., Factors affecting the creep strength of magnesia refractories. *Br. Ceram. Trans. J.*, **84** (1985) 108–10.
13. Wiederhorn, S. M. & Krause, R. F., Effect of coal slag on the microstructure and creep behavior of a magnesium–chromite refractory. *Am. Ceram. Soc. Bull.*, **67** (1988) 1201–10.
14. Pandolfelli, V. C., Salvini, V. R., Brant, P. O. R. C., Noronha, R. T. T. & Mattos, U., Influence of mullite zirconia aggregate addition on the thermomechanical properties of high-alumina refractories. *Proc. Unified International Technical Conference on Refractories — UNITECR 93*, ed. Alafar, São Paulo, Brazil, 1993, pp. 282–91.
15. *Phase Diagrams for Ceramists*, ed. M. K. Reser. The American Ceramic Society, Columbus, USA, 1980.
16. Kingery, W. D., Bowen, H. K., & Uhlmann, D. R., *Introduction to Ceramics*. 2nd Edition, John Wiley & Sons, New York, 1976, p. 589 f.
17. Dörre, E. & Hübner, H., *Alumina. Processing, Properties and Applications*. Springer-Verlag, Berlin, 1984, pp. 154–73.
18. Monkman, F. C. & Grant, N. J., An empirical relationship between rupture and minimum creep rate in creep-rupture tests. Proc. *ASTM*, **56** (1956) 593–620.
19. Chien, Y. T., Lee, T. F., Pan, H. C. & Ko, Y. C., Effect of Cr_2O_3 on creep resistance of high alumina bauxite refractories. *Am. Ceram. Soc Bull.*, **63** (1984) 915–18.
20. Hou, L. D. & Kröger, F. A., Creep in Polycrystalline Al_2O_3: Si. *Mater. Sci. Lett.*, **3** (1984) 993–6.